

NANO EXPRESS

Open Access

Gas sensing properties of conducting polymer/ Au-loaded ZnO nanoparticle composite materials at room temperature

Viruntachar Kruefu^{1*}, Anurat Wisitorsaet², Adisorn Tuantranont² and Sukon Phanichphant³

Abstract

In this work, a new poly (3-hexylthiophene):1.00 mol% Au-loaded zinc oxide nanoparticles (P3HT: Au/ZnO NPs) hybrid sensor is developed and systematically studied for ammonia sensing applications. The 1.00 mol% Au/ZnO NPs were synthesized by a one-step flame spray pyrolysis (FSP) process and mixed with P3HT at different mixing ratios (1:1, 2:1, 3:1, 4:1, and 1:2) before drop casting on an Al₂O₃ substrate with interdigitated gold electrodes to form thick film sensors. Particle characterizations by X-ray diffraction (XRD), nitrogen adsorption analysis, and high-resolution transmission electron microscopy (HR-TEM) showed highly crystalline ZnO nanoparticles (5 to 15 nm) loaded with ultrafine Au nanoparticles (1 to 2 nm). Film characterizations by XRD, field-emission scanning electron microscopy (FE-SEM), energy-dispersive X-ray (EDX) spectroscopy, and atomic force microscopy (AFM) revealed the presence of P3HT/ZnO mixed phases and porous nanoparticle structures in the composite thick film. The gas sensing properties of P3HT:1.00 mol% Au/ZnO NPs composite sensors were studied for reducing and oxidizing gases (NH₃, C₂H₅OH, CO, H₂S, NO₂, and H₂O) at room temperature. It was found that the composite film with 4:1 of P3HT:1.00 mol% Au/ZnO NPs exhibited the best NH₃ sensing performances with high response (approximately 32 to 1,000 ppm of NH₃), fast response time (4.2 s), and high selectivity at room temperature. Plausible mechanisms explaining the enhanced NH₃ response by composite films were discussed.

Keyword: P3HT; Au-loaded ZnO; Composite films; NH₃ sensor; Flame spray pyrolysis

Background

Gas sensors for ammonia (NH₃) detection at low concentration are of great scientific importance in environmental monitoring, medical diagnosis, and various chemical/agricultural industries, since ammonia is very harmful to humans and the environment [1-5]. Several semiconducting metal oxides are highly promising for NH₃ detection due to their excellent response [6-8]. However, they suffer from some inconvenience including high operating temperatures (200°C to 400°C) [6-11]. High operating temperature results in high power consumption and complicated sensor design/fabrication [12]. Thus, ammonia sensors operable at room temperature with long life time are of great interest.

Conducting polymers, such as polypyrrole (PPy), polyaniline (Pani), polythiophene (PTh), and their derivatives, have demonstrated gas sensing capability at low or even room temperature [13,14]. However, they are still not practically useful due to comparatively low response, lack of specificity, and relatively poor stability. A summary of gas sensing properties of NH₃ gas sensor-based conducting polymers as well as their hybrids prepared by various methods is shown in Table 1. Firstly, polyaniline (PANI) nanowires (NWs) prepared by photolithography process are shown to exhibit a high sensor response of approximately 3 at 500 ppm NH₃ in synthetic air [14]. In addition, surface acoustic wave (SAW) NH₃ gas sensors based on PPy prepared by layer-by-layer (LBL) self-assembly method are investigated for NH₃ sensing with different numbers of layer. The sensor with two layers of PPy shows the best performance relative to those with other numbers of PPy layers [15]. Additionally, NH₃ gas sensors based on organic thin-film transistors (OTFTs) made from spin-coated poly

* Correspondence: v_viruntachar@hotmail.com

¹Program in Materials Science, Faculty of Science, Maejo University, Chiang Mai 50290, Thailand

Full list of author information is available at the end of the article

Table 1 Summary of NH₃ sensing properties of a conducting polymer and metal or metal oxide/conducting polymer sensor

Authors/reference	Method	Materials	NH ₃ concentration (ppm)	NH ₃ sensing performances
Chen et al. [15]	Layer-by-layer (LBL) self-assembly method	Polypyrrole (PPy) and Pt-doped two-layer PPy thin films	100	Response: approximately 3 to 100 ppm NH ₃ at room temperature
Jeong et al. [16]	Spin coating	P3HT thin-film transistors	10 to 100	Response: 0.31 to 100 ppm NH ₃ at room temperature
Saxena et al. [27]	Drop casting	P3HT:ZnO nanowire thin films	4	Response: <1% to 4 ppm NH ₃ at room temperature
Chougule et al. [13]	Low-frequency AC spin coating	CSA (30 wt.%) doped PPy-ZnO hybrid films	100	Response: approximately 11 to 100 ppm NH ₃ at room temperature
Baratto [18]	Drop casting	Hybrid poly (3-hexylthiophene)-ZnO nanocomposite thin films	25	Response: small response to 25 ppm NH ₃ at room temperature
Tuan et al. [14]	A standard photolithography technique	Polyaniline (PANI) nanowires (NWs)	25 to 500	Response: 2.9 to 500 ppm NH ₃ at room temperature
Tai et al. [21]	<i>In situ</i> self-assembly	Polyaniline/titanium dioxide (PANI/TiO ₂) nanocomposite thin films	23 to 141	Response: approximately 9 to 140 ppm NH ₃ , response time 2 s, and recovery time 20 to 60 s at room temperature
Huang et al. [26]	Spin coating	Graphene oxide (RGO)-polyaniline (PANI) hybrids	50	Response: approximately 10.4 to 50 ppm NH ₃ at room temperature
Dhingra et al. [23]	Dipping	Zinc oxide/polyaniline (ZnO/PANI) hybrid	300	Response: approximately 23 to 300 ppm NH ₃ at room temperature
This work	Drop casting	P3HT:1.00 mol% Au/ZnO NPs (4:1)	50 to 1,000	Response: approximately 32 to 1,000 ppm NH ₃ at room temperature

(3-hexylthiophene) (P3HT) on a thermally grown SiO₂/Si wafer exhibit a sensor response of 0.31 to 100 ppm NH₃ at room temperature [16]. Among these, P3HT is particularly promising for gas sensing applications due to its selective room-temperature response toward some gases especially ammonia and NO₂ [16-18] and its relatively high stability. P3HT is known to have high oxidation potential making it highly stable in doped/undoped states under ambient conditions at room temperature and has specific chemical interactions with some gases [17].

The advantages of organic materials can be further exploited by their combinations with metal oxides [13,18-23] and metals [15,19,24,25]. For instance, the hybrid of graphene oxide (GO)-polyaniline (PANI) nanoparticles prepared by spin coating is shown to exhibit higher response to 50 ppm of NH₃ than those of bare PANI nanofiber and bare GO sensors by a factor of 3.4 and 10.4, respectively [26]. In addition, P3HT/ZnO NWs and polypyrrole-zinc oxide (PPy-ZnO) composites are reported for sensitive detection of NH₃ [13,27]. In contrast, another report of P3HT-ZnO NW thin films demonstrates high sensitivity for NO₂ or H₂S and a moderate sensitivity for CO [27], while the response to NH₃ was very low ($S < 1%$) at room temperature. Furthermore, PPy-ZnO hybrid films are doped with camphor sulfonic acid (30 wt.%) and exhibit high selectivity to NO₂, high sensitivity at low NO₂ concentration (80% to 100 ppm), fast response time (120 s), and good stability but relatively sluggish response to reducing gases

(H₂S, NH₃, C₂H₅OH, and CH₃OH) at room temperature [13]. Moreover, novel P3HT-ZnO nanocomposite hybrid thin films show a high relative response of 2.2 to 200 ppb of NO₂ but virtually no response to CO or C₂H₅OH and very small response to NH₃ at room temperature [18]. Besides, zinc oxide/polyaniline (ZnO/PANI) hybrid structures are confirmed to exhibit much higher sensitivity to NH₃ gas at room temperature than bare ZnO [23,28].

It can be observed that ZnO nanostructures are among the most widely employed metal oxides in polymer-based hybrid gas sensors, which should be due to its observed gas sensing enhancement, abundance, low cost, high stability, high electron mobility, low crystallization temperature, and ease of fabrication. However, mechanisms for gas sensing enhancement provided by ZnO nanostructures are not yet well understood. Nevertheless, it is widely observed that sensing properties of the hybrid sensors are related to surface characteristics of ZnO, which significantly depend on fabrication processes [29]. Most reported work mostly employs chemical-route and chemical vapor deposition (CVD) methods, which suffer from either poor reproducibility or high cost. Alternative low-cost, effective, and reliable methods for mass production of metal oxide nanostructured components in composite are still needed. Flame spray pyrolysis (FSP) is one of the most promising routes for the formation of single and multi-component functional nanoparticles with well-controlled diameter at low cost and high production rate. FSP has been applied to prepare metal oxide-

supported nanoparticles and heterogeneous catalysts. However, FSP-made materials have not been employed in polymer-metal oxide hybrid sensors. It is thus interesting to apply them in this sensor system.

Gold (Au) is another effective means to improve sensing performance of polymer-based gas sensors via catalytic effects, which may be attained at low or room temperature. For instance, Pd incorporation in PANI considerably improved the response to methanol [19]. Similarly, Pt loading in PPy gas-sensitive films considerably improved NH₃ responses of the PPy sensor [15]. Au is another effective catalyst for gas sensing [30]. Au loading on metal oxides particularly ZnO nanostructures has demonstrated to enhance response toward C₂H₅OH [31] and CO [30]. However, Au is relatively much less employed in polymer-based hybrid gas sensors. Its effect on gas sensing of a polymer-based hybrid sensor should thus be investigated.

Furthermore, the combination of noble metal catalyst, metal oxide, and polymer is expected to offer superior room-temperature gas sensors. To date, there has been development of noble metal/metal oxide/polymer composite gas sensors. In this work, we propose a practical implementation of this approach by blending a P3HT conductive polymer with Au-loaded ZnO nanoparticles (NPs) prepared by FSP. The novel hybrid materials are structurally characterized and tested for ammonia detection. In addition, the effects of ZnO and gold loading on gas sensing properties of P3HT sensing films are systematically analyzed by comparing the performances of P3HT with and without unloaded and 1.00 mol% Au-loaded ZnO NPs.

Methods

Synthesis and characterization of nanoparticles

The 1.00 mol% Au-loaded ZnO nanoparticles (Au/ZnO NPs) were successfully synthesized by the FSP process schematically illustrated in Figure 1. The precursor solution for FSP was prepared from zinc naphthenate (Sigma-Aldrich, St. Louis, MO, USA; 8 wt.% Zn) and gold (III)-chloride hydrate (Sigma-Aldrich; ≥49% Au) diluted in ethanol (Carlo Erba Reagenti SpA, Rodano, Italy; 98.5%). The precursor solution was injected at 5 mL min⁻¹ through the reactor nozzle and dispersed with 5.0 L min⁻¹ of oxygen into a fine spray (5/5 flame) while maintaining a constant pressure drop of 1.5 bar across the nozzle tip. A premixed flame fueled by 1.19 L min⁻¹ of methane and 2.46 L min⁻¹ of oxygen was ignited and maintained to support the combustion of the spray. The flames have yellowish orange color with a height of approximately 10 to 11 cm for both unloaded ZnO and 1.00 mol% Au/ZnO as shown in Figure 1.

Upon evaporation and combustion of precursor droplets, particles are formed by nucleation, condensation,

coagulation, coalescence, and Au deposition on a ZnO support. Finally, the nanoparticles were collected from glass microfiber filters (Whatmann GF/D, 25.7 cm in diameter) placed above the flame with an aid of a vacuum pump. X-ray diffraction (TTRAXIII diffractometer, Rigaku Corporation, Tokyo, Japan) was employed to confirm the phase and crystallinity of obtained nanoparticles using CuKα radiation at 2θ = 20° to 80° with a step size of 0.06° and a scanning speed of 0.72°/min. Brunauer-Emmett-Teller (BET) analysis by nitrogen absorption (Micromeritics Tristar 3000, Micromeritics Instrument Co., Norcross, GA, USA) at liquid nitrogen temperature (77.4 K) was performed to obtain the specific surface area of the nanoparticles. The average particle size (d_{BET}) in nanometers is equal to $6/(SSA_{\text{BET}} \times \rho_{\text{av}})$, where SSA_{BET} is the specific surface area (m²/g) and ρ_{av} is the average density of the flame-made 1.00 mol% Au/ZnO NPs with $\rho_{\text{ZnO}} = 5.606 \text{ g cm}^{-3}$ [32,33] and $\rho_{\text{Au}} = 19.32 \text{ g cm}^{-3}$ [24], which took into account their weight content. High-resolution transmission electron microscopy (HR-TEM) was employed to examine the morphology and size of nanoparticles. The elemental composition of nanoparticles was analyzed by energy-dispersive X-ray spectroscopy (EDX) in mapping mode to confirm Au content in the resultant powders.

Sensor fabrication and sensing film characterization

Composite sensors were prepared by blending P3HT (Rieke Metals, Inc., Lincoln, NE, USA; M_w 48,000 g mol⁻¹) solution with 1.00 mol% Au/ZnO NP colloidal solution and drop casting onto prefabricated Cr/Au interdigitated electrodes. Cr (50 nm thick) and Au (200 nm thick) layers were deposited by DC sputtering in argon gas at a pressure of 3×10^{-3} mbar on an alumina substrate (0.40 cm × 0.55 cm × 0.04 cm). The interdigit spacing, width, and length were 100 μm, 100 μm, and 0.24 cm, respectively. P3HT solution was prepared by dissolving 30 mg of P3HT in 0.50 mL of chlorobenzene, and Au/ZnO NP colloidal solution was made by dispersing 5 to 25 mg of ZnO nanoparticles (unloaded ZnO and 1.00 mol% Au/ZnO) in 0.50 mL of 1-butanol.

To prepared hybrid films with various compositions, 1.00 mol% Au/ZnO NP colloidal solution was added to the stirred P3HT solution with five different mixing ratios (1:1, 2:1, 3:1, 4:1, and 1:2). The blended solution was drop casted on the interdigitated electrode and then baked at 150°C for 3 min in an oven. The active area of these sensing devices is $0.12 \pm 0.04 \text{ cm}^2$. After completion, the crystalline phase of composite films was characterized by X-ray diffraction (XRD). The surface morphologies, elemental analysis, and cross section of the sensing layers were verified by field-emission scanning electron microscopy (FE-SEM) equipped with an EDX analysis system. Finally, the devices were transferred to a

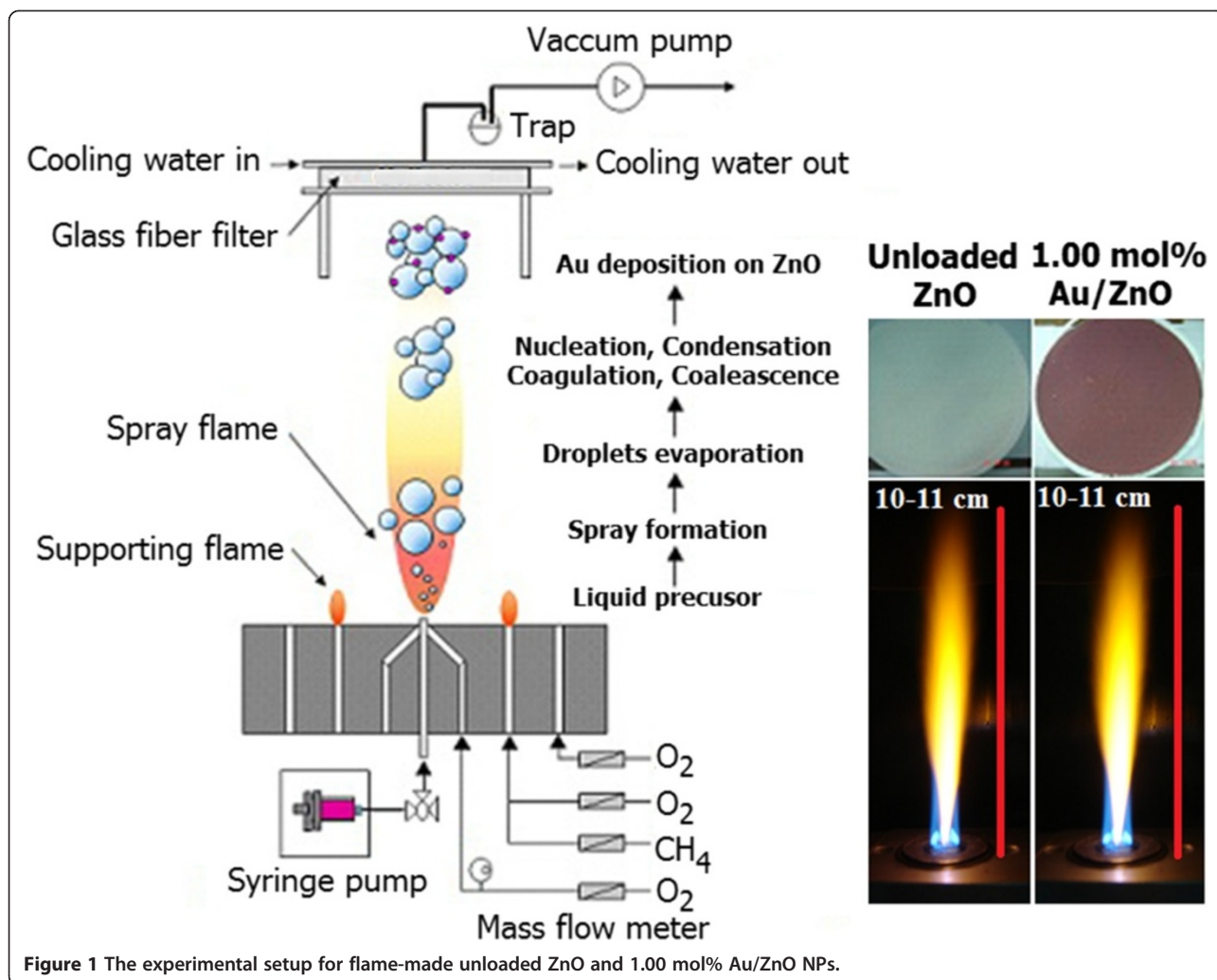


Figure 1 The experimental setup for flame-made unloaded ZnO and 1.00 mol% Au/ZnO NPs.

stainless steel chamber for gas sensing measurement at room temperature.

Electrical and sensing test

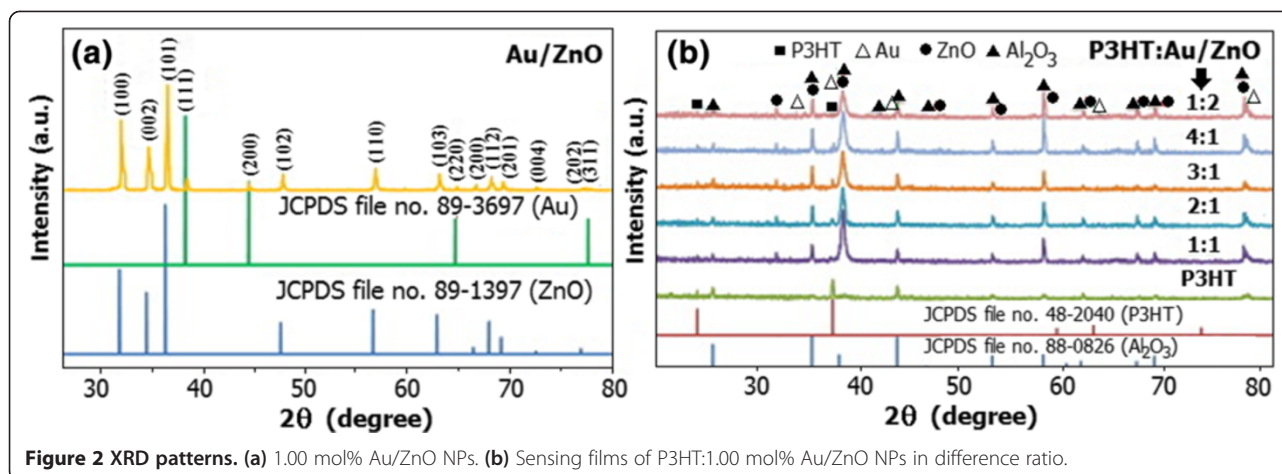
P3HT and P3HT:1.00 mol% Au/ZnO NPs sensors were then tested by the standard flow through method in a stainless steel chamber at room temperature (25°C). The sensing experiment was carried out by measuring the reversible change of electrical resistance of sensors taken through a 6517 Keithley resistance meter (Keithley Instruments Inc., Cleveland, OH, USA) under a DC applied voltage of 10 V. A constant flux of synthetic dry air of 1 L/min as gas carrier was flowed to mix with the desired concentration of pollutants dispersed in synthetic air, and gas flow rates were precisely manipulated using a computer-controlled multi-channel mass flow controller. The background relative humidity (RH) under a flux of dry air was measured to be around 10%. The NH₃ pollutant source is a calibrated ammonia vapor

balanced in dry air at 4,000 ppm (Linde Co. Ltd, Bangkok, Thailand). Ammonia (NH₃) vapor concentration was varied from 25 to 1,000 ppm. The gas sample exposure time and the dry air restoring time were fixed at 10 and 25 min, respectively. For selectivity performance, the sensors were also tested toward C₂H₅OH, CO, H₂S, and NO₂ at 1,000 ppm. The effect of humidity was also tested at 80% RH.

Results and discussion

Particles and sensing film properties

The XRD pattern of 1.00 mol% Au/ZnO NPs as shown in Figure 2a reveals that the nanoparticle is highly crystalline and has the hexagonal structure of ZnO according to JCPDS no. 89-1397. Au peaks are also found in these patterns and well matched with a face-centered cubic phase of Au (JCPDS file no. 89-3697 [34]). The XRD patterns of P3HT and P3HT:1.00 mol% Au/ZnO NPs composite sensing films coated on Au/Al₂O₃ substrates in Figure 2b



indicate the presence of the P3HT monoclinic crystal (the JCPDS no. 48–2040), the hexagonal ZnO phase of the NPs, a fcc phase of Au (JCPDS file no. 89–3697 [34]), and a corundum phase of Al₂O₃ (JCPDS file no. 88–0826 [35]). It can be seen that Au peaks of the hybrid film are relatively pronounced compared with those of 1.00 mol% Au/ZnO NPs. These observed Au peaks are mainly attributed to the diffraction from the interdigitated Au electrode, which almost completely overrides the very weak diffraction from Au loaded on ZnO NPs.

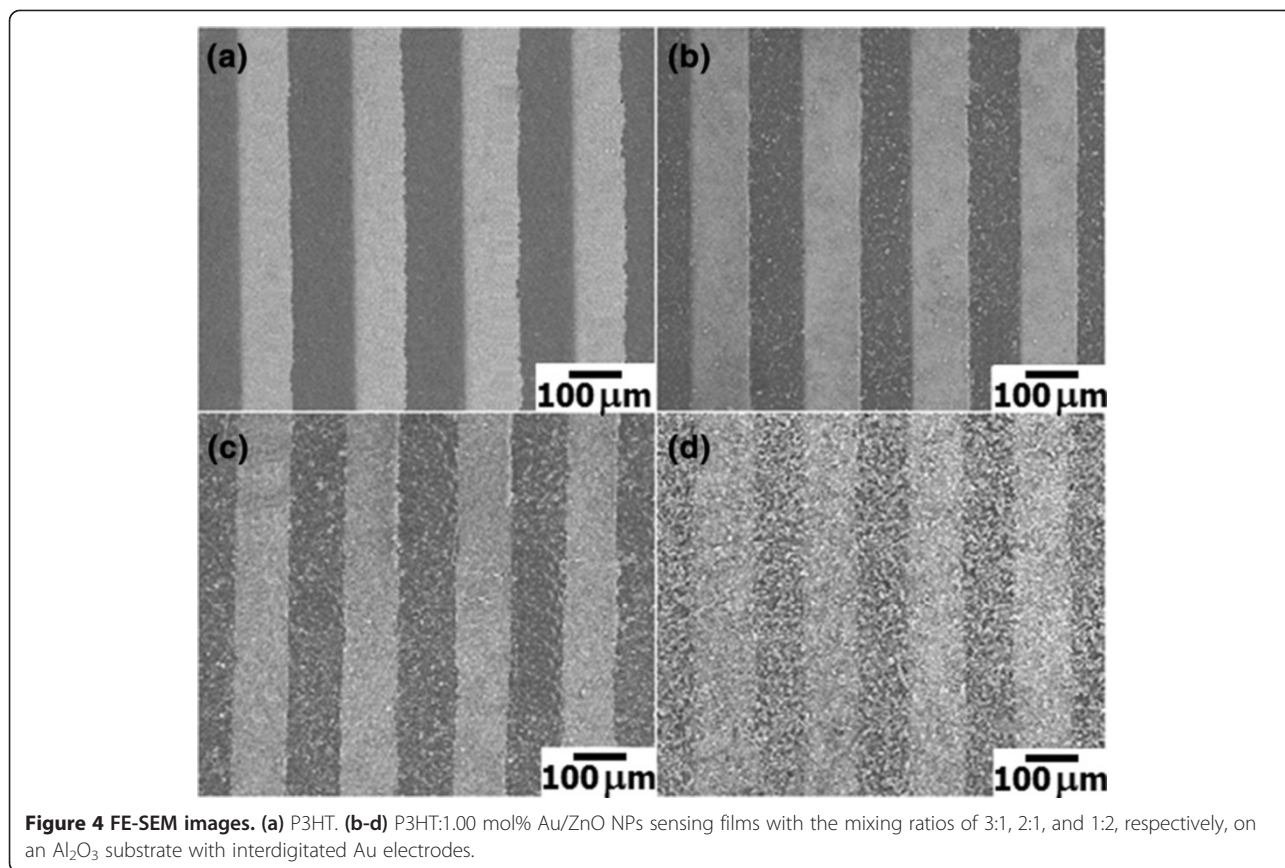
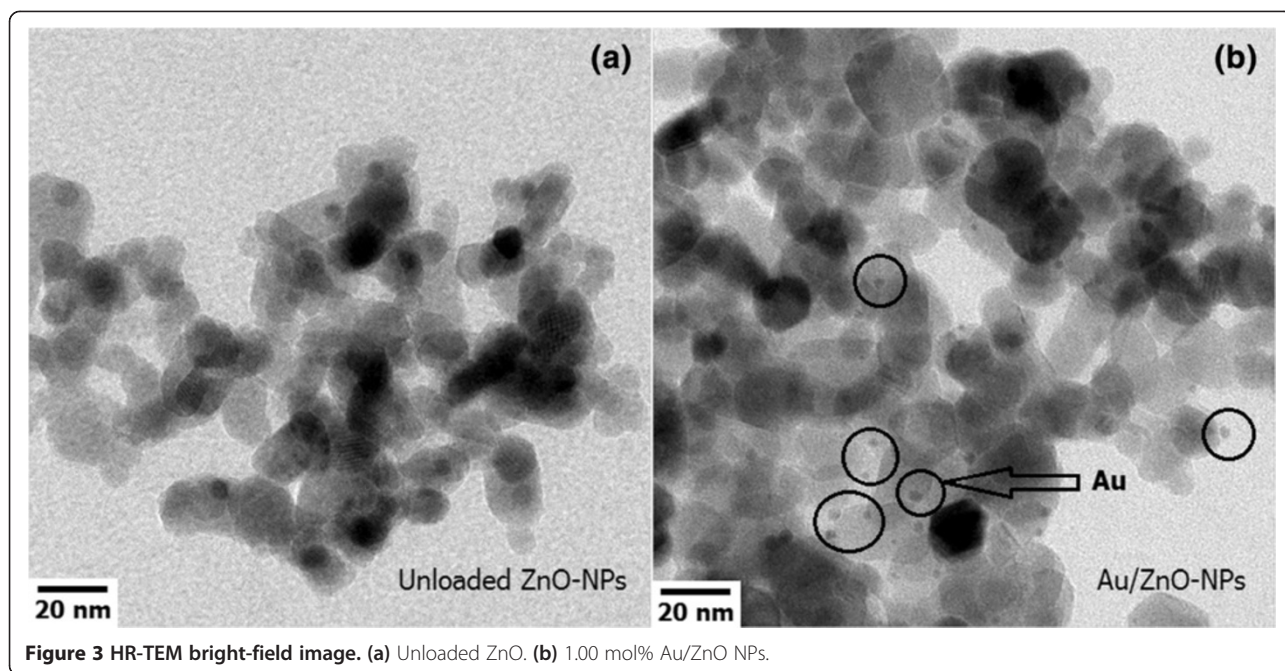
The specific surface area of the unloaded ZnO and 1.00 mol% Au/ZnO NPs was measured by nitrogen absorption using BET analysis. It was found that the specific surface area (SSA_{BET}) of unloaded ZnO and 1.00 mol% Au/ZnO NPs is about 86.3 and 100 m² g⁻¹, respectively. The corresponding BET equivalent particle diameters (d_{BET}) of unloaded ZnO and 1.00 mol% Au/ZnO NPs are calculated to be about 10 and 9 nm, respectively. Thus, 1.00 mol% Au loading on ZnO NPs increases the specific surface area by 15% and reduces the particle diameter by about 10%. HR-TEM images of unloaded ZnO and 1.00 mol% Au/ZnO NPs in Figure 3 show spherical nanoparticles along with a few nanorods having a size in the range of 5 to 15 nm. For Au-loaded ZnO (Figure 3b), smaller spherical NPs with an average diameter of approximately 1.5 nm are clearly observed on the surface of ZnO as the darker spots as indicated in the figure. These NPs are confirmed to be Au NPs on ZnO support by EDX analysis in mapping mode (data not shown). The observed particle diameters by HR-TEM are in the same range as BET data. The observed smaller Au nanoparticle diameter of approximately 1.5 nm explains the result that the average BET nanoparticle diameter becomes smaller with Au loading as the average particle size will be reduced by the contribution of smaller particles.

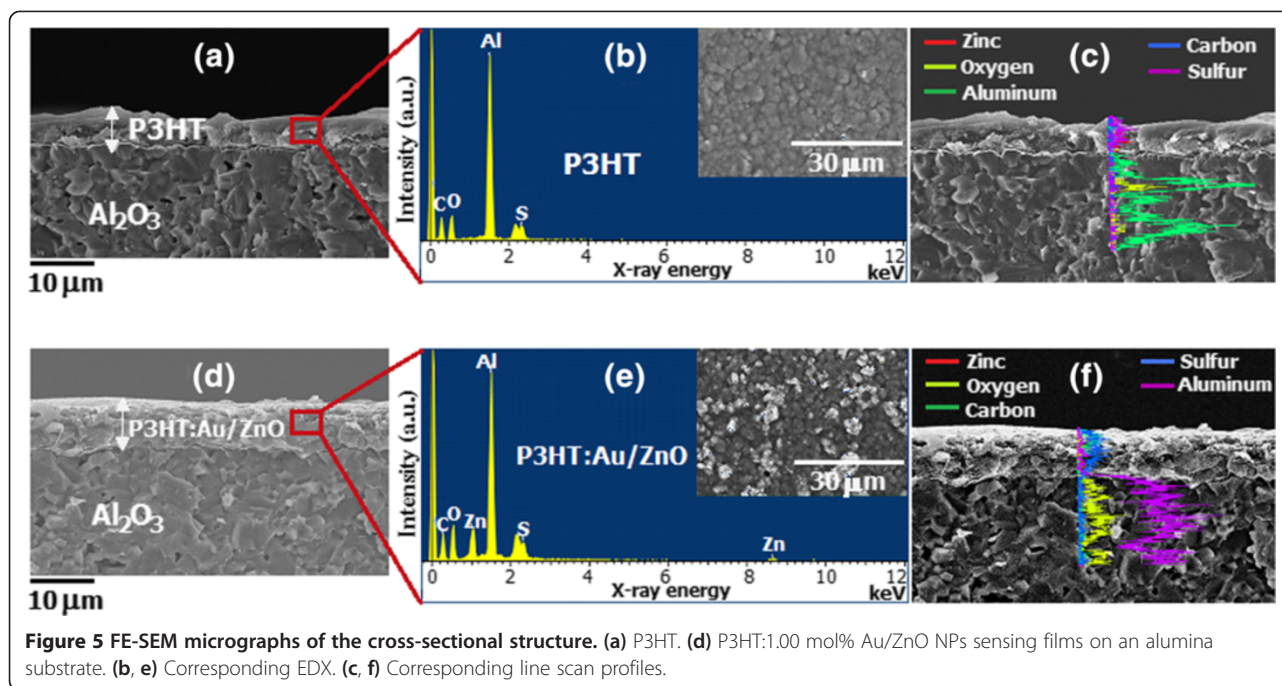
Figure 4 shows FE-SEM images of P3HT and P3HT: 1.00 mol% Au/ZnO NPs composite sensing films with

the ratios of 4:1, 2:1, and 1:2 deposited on Al₂O₃ substrates with interdigitated Au electrodes. It can be seen that the surface of P3HT film is smooth and conformal with Au lines of the interdigitated electrode (Figure 4a). Upon mixing with 1.00 mol% Au/ZnO NPs, the surface becomes a relatively rough covering with fine white spots of NPs. The distribution of these spots on the Au interdigitated electrode surface is quite uniform, and the density of white spots increases accordingly with increasing content of NPs (Figure 4b, c, d). The results confirm the homogenous dispersion of 1.00 mol% Au/ZnO NPs in the P3HT matrix and its conformal coating on the substrate. In addition, the specific surface area of the composite film should be increased with increasing content of 1.00 mol% Au/ZnO NPs.

The cross-sectional FE-SEM images along with EDX analyses of P3HT and P3HT:1.00 mol% Au/ZnO NPs (4:1) composite sensing films on an Al₂O₃ substrate with interdigitated Au electrodes after sensing test at room temperature in dry air are illustrated in Figure 5. It can be seen that the P3HT film is a smooth and solid layer (Figure 5a, b, c), while the composite film demonstrates porous asperities of the nanoparticle-polymer mixture (Figure 5d, e, f). The thicknesses of P3HT and composite films are estimated in the same range of 6 to 8 μm. The elemental composition on the surface and across P3HT and P3HT:1.00 mol% Au/ZnO NP layers is demonstrated in the EDX spectra and line scan profiles (Figure 5b, c and 5e, f, respectively). It confirms that the P3HT film contains only oxygen (O), carbon (C), and sulfur (S) and the P3HT:1.00 mol% Au/ZnO NP layer has one additional element of zinc (Zn) while the gold (Au) loaded element cannot be observed due to its very low content. In addition, the line scan profiles indicate that elemental compositions through the films are quite uniform.

Atomic force microscopy (AFM) was employed to quantitatively investigate the morphology of P3HT and





P3HT:1.00 mol% Au/ZnO NPs (4:1) composite sensing films drop casted on the Al_2O_3 substrate (Figure 6). The results indicate that the film surfaces are quite uniform, containing only tiny defects within a scan area of $20 \mu\text{m} \times 20 \mu\text{m}$. The average surface roughness of P3HT and the P3HT:1.00 mol% Au/ZnO NPs film is calculated from AFM data to be 130.1 and 135.2 nm, respectively. In addition, the composite film exhibits a relatively sharp granular morphology with a uniform grain size of approximately 80 to 100 nm, suggesting the presence of a nanosized grain structure in the composite sensing film due to the addition of 1.00 mol% Au/ZnO NPs.

Gas sensing properties

The dynamic changes in resistance of sensors with different mixing ratios of P3HT:1.00 mol% Au/ZnO NPs (1:0, 1:1, 2:1, 3:1, 4:1, 1:2, and 0:1) are shown in Figure 7. It is seen that all sensors exhibit an increase of resistance during NH_3 exposure, indicating a p-type-like gas sensing behavior. In addition, it is observed that the baseline resistance monotonically increases with increasing content of 1.00 mol% Au/ZnO NPs in accordance with the typical combination of materials' resistances. Furthermore, P3HT exhibits a moderate NH_3 response, while 1.00 mol% Au/ZnO NPs give very low response to NH_3 at room temperature. Moreover, the addition of 1.00 mol% Au/ZnO NPs into P3HT at a mixing ratio up to 1:1 leads to significant enhancement in the NH_3 response compared with the P3HT sensor. However, the response rapidly degrades when the amount of 1.00 mol% Au/ZnO NPs exceeds that of P3HT (1:2).

From calculated changes of resistance, it is found that the sensor with 4:1 of P3HT:1.00 mol% Au/ZnO NPs exhibits the highest value, indicating that it is the optimal P3HT:1.00 mol% Au/ZnO NPs composite sensor. Since the optimal mixing ratio of the Au/ZnO NPs and P3HT of 1:4 is at the lowest border of the investigated range, it is possible that the actual optimal concentration will be at a lower concentration value and further detailed investigation should be conducted to refine the result. The obtained optimal performances of P3HT: Au/ZnO sensors are superior to other reports presented in Table 1 with a relatively high response magnitude of 32 and wide concentration range of 1,000 ppm. However, the response at lower concentration may be lower than some work such as ZnO/PANI hybrid [23] and PANI/ TiO_2 nanocomposite thin films [21].

The sensor characteristics are then analyzed in terms of sensor response and response time. The sensor response (S) is determined from the electrical resistance change of P3HT:1.00 mol% Au/ZnO NPs sensors upon exposure to target gas using the following relation: $S = R_{\text{gas}}/R_{\text{air}}$ where R_{gas} and R_{air} are the stable electrical resistance of a sensor upon exposure to NH_3 and the initial resistance in air, respectively. The response time is defined as the time needed for a sensor to attain 90% of maximum change in resistance upon exposure to a test gas. The calculated sensor response and response time of optimal sensors with 4:1 of P3HT:1.00 mol% Au/ZnO NPs are shown in Figure 8. Apparently, the sensor response to NH_3 gas monotonically increases upon exposure with increasing NH_3 concentration from 25 to

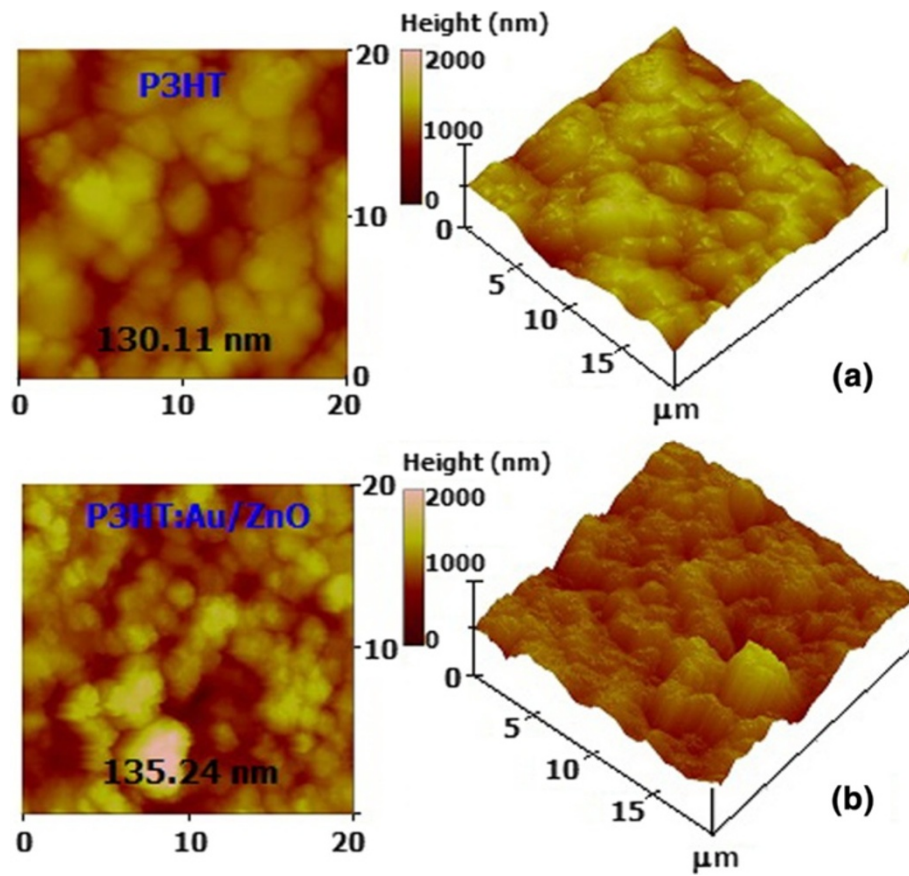


Figure 6 AFM morphology. (a) P3HT. (b) P3HT:1.00 mol% Au/ZnO NPs (4:1) hybridized sensing film drop casted on an Al₂O₃ substrate.

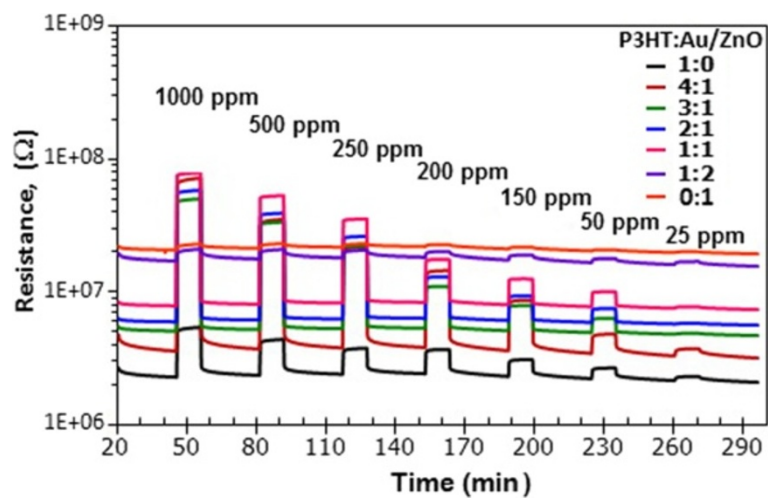
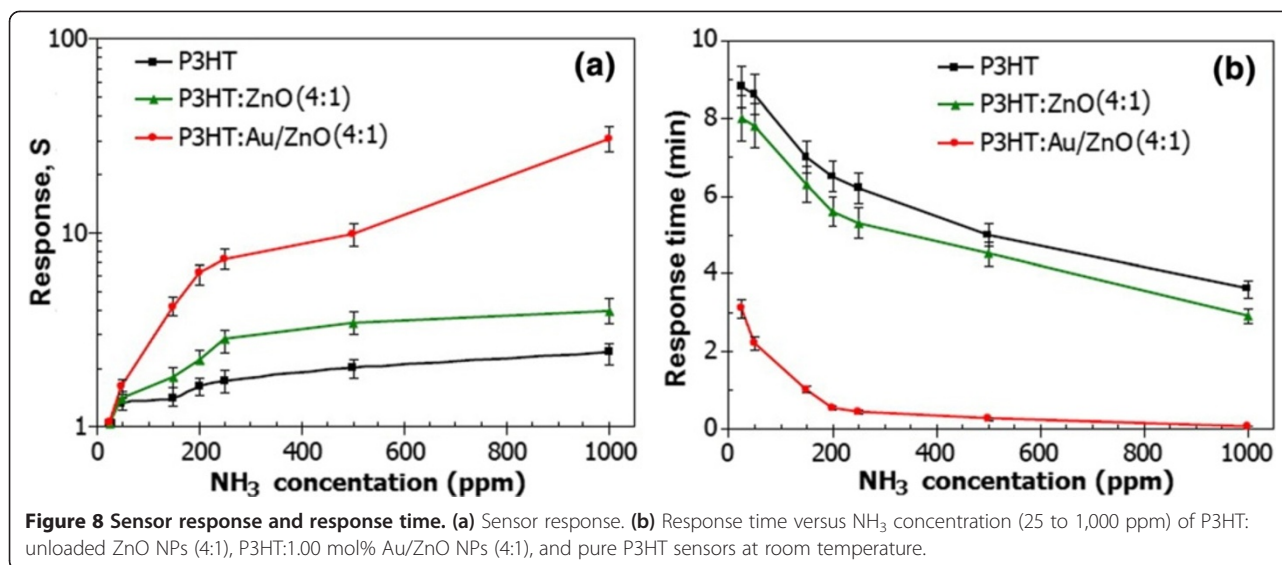


Figure 7 Change in resistance. The resistance of sensors with difference ratio of P3HT:1.00 mol% Au/ZnO NPs (1:0, 1:1, 2:1, 3:1, 4:1, 1:2, and 0:1) toward 25 to 1,000 ppm NH₃ at room temperature.



1,000 ppm. At 1,000 ppm, the composite sensor prepared with the 4:1 ratio exhibits the highest NH₃ response of 32 and a short response time of 4.2 s. Thus, 1.00 mol% Au/ZnO NPs:P3HT composite sensors offer excellent NH₃ sensing performances with high response, short response time, and room-temperature operation. It should be noted that γ -error bars of all data correspond to the statistical spread from five sensors of each composition with five evaluations. The statistical results show that fabricated composite sensors offer good repeatability and reproducibility with maximum variation of less than 20%.

The enhanced gas sensing response of the P3HT: 1.00 mol% Au/ZnO NPs (4:1) composite sensor may be attributed to the high specific surface area of P3HT surface-coated on granular 1.00 mol% Au/ZnO, which enhances gas adsorption and interaction at the interface [13,21,36]. In order to distinguish the roles of ZnO and gold nanoparticles, the NH₃ sensing performances of P3HT:ZnO loaded with Au (4:1) are compared with those of P3HT:unloaded ZnO (4:1) and pure P3HT as also demonstrated in Figure 8. It can be seen that the response of the P3HT sensor is only slightly improved by the addition of unloaded ZnO at the mixing ratio of 4:1, while Au addition by loading on ZnO NPs leads to significant increase of NH₃ response by almost an order of magnitude. In addition, the response time is also substantially reduced to a few minutes or seconds, while ZnO addition does not notably decrease the response time. Thus, Au plays a much more important role than ZnO NPs in enhancing NH₃ response of the composite sensor. Moreover, it was found from our preliminary study that NH₃ response of the P3HT:Au-loaded ZnO film increased monotonically as Au loading level increased from 0 to 1.00 mol%. Thus, if Au content

increased further, the NH₃ response should increase to an optimal point and then reduce due to particle aggregation. Further study will be conducted to determine the ultimate optimal Au loading level of the P3HT:flame-made Au-loaded ZnO film for NH₃ sensing and fully reported elsewhere.

The gas sensing mechanism for the composite sensors may be explained on the basis of interactions between the sensing film and adsorbed gas. For pure P3HT, it has been proposed that NH₃ can adsorb and donate a lone pair of its electrons to the pentagonal sulfur ring in the P3HT structure [22]. Electrons will recombine with existing holes in the p-type P3HT, leading to a resistance increase in agreement with the observed NH₃ response. By adding unloaded ZnO NPs, the response is enhanced by a factor of approximately 1.5. This could reasonably be explained by the increase of specific surface area for gas interaction of the composite film by ZnO NPs. From the FE-SEM image in Figure 5, ZnO NP addition results in considerable increase of film porosity and hence the surface area. However, the magnitude of this increase cannot be quantitatively confirmed as BET measurement, which is currently the only quantitative analysis method of specific surface area, of the film surface is presently not available because the standard BET method requires a large amount of material (>0.3 g) which is difficult to prepare in the form of film and the presence of substrate will considerably complicate nitrogen adsorption evaluation. Thus, the specific surface area of the composite film can only be inferred from BET data of the corresponding powder and SEM images.

With Au loading, the response is enhanced much more drastically than ZnO NPs and the response also increases with increasing Au loading level from 0 to 1.00 mol%. Considering the effect of surface area change,

the BET specific surface area of ZnO NPs is found to increase from 86.3 to 100 m² g⁻¹ with 1.00 mol% Au loading (see the 'Particles and sensing film properties' section). This corresponds to the 15.9% increase, and the influence of specific surface area alone cannot explain the observed large response enhancement by Au loading on ZnO. From the results, Au loading on ZnO increases not only the response magnitude but also the response rate substantially. Thus, the most plausible mechanism for such enhancement should be the catalytic effect of Au on ZnO NPs. Figure 9 depicts our proposed model for the catalytic effect of Au/ZnO NPs based on a P3HT-ammonia interaction mechanism reported recently [17]. In this model, it is assumed that Au/ZnO NPs located around sulfur atoms in the pentagonal rings of P3HT catalyze the reaction, causing more NH₃ molecules to give lone-pair electrons and form the weak binding. The probability for Au/ZnO NPs should be high since gold and sulfur have rather strong binding affinity. To obtain effective catalyst activity, Au NPs should be uniformly dispersed throughout the P3HT matrix. Thus, Au plays the main role in enhancing NH₃ interaction and response with P3HT, while the role of ZnO NPs is the supports that help formation and dispersion of ultrafine Au nanoparticles. However, when only 1.00 mol% Au/ZnO is used, there is no response since Au catalyzes the reaction between NH₃ and P3HT.

For the effect of composite composition, the results show that 4:1 of P3HT:1.00 mol% Au/ZnO NPs, which is the composite with the lowest 1.00 mol% Au/ZnO NP content, offers the highest NH₃ sensing enhancement and the enhancement decreases with increasing Au/ZnO NP content. A plausible explanation is that 1.00 mol% Au/ZnO NPs are well dispersed in the P3HT matrix at this low concentration, yielding a homogeneous distribution of Au/ZnO NPs throughout the layer and enabling effective catalytic interaction with NH₃ gas. In addition, the well-dispersed structure should be highly porous and exhibit large surface area for gas interaction. As the content of 1.00 mol% Au/ZnO NPs increases, the Au/ZnO NPs may begin to agglomerate resulting in less homogenous formation of Au/ZnO NPs and less porous composite structures, which lead to low NH₃ sensing response. Based on the current results, NH₃ sensing properties of the composite film may be further improved by optimizing the structure/composition of the Au loading material as well as metal oxide support to maximize the catalytic effect and by adding intercalating nanomaterials with different dimensionalities (i.e., 2D graphene, 1D metal oxide nanowire, 1D carbon nanotubes, etc.) to reduce particle agglomeration and increase effective surface area. Moreover, new catalysts based on the composite of Au and other catalytic materials should be explored to further improve the catalytic effect.

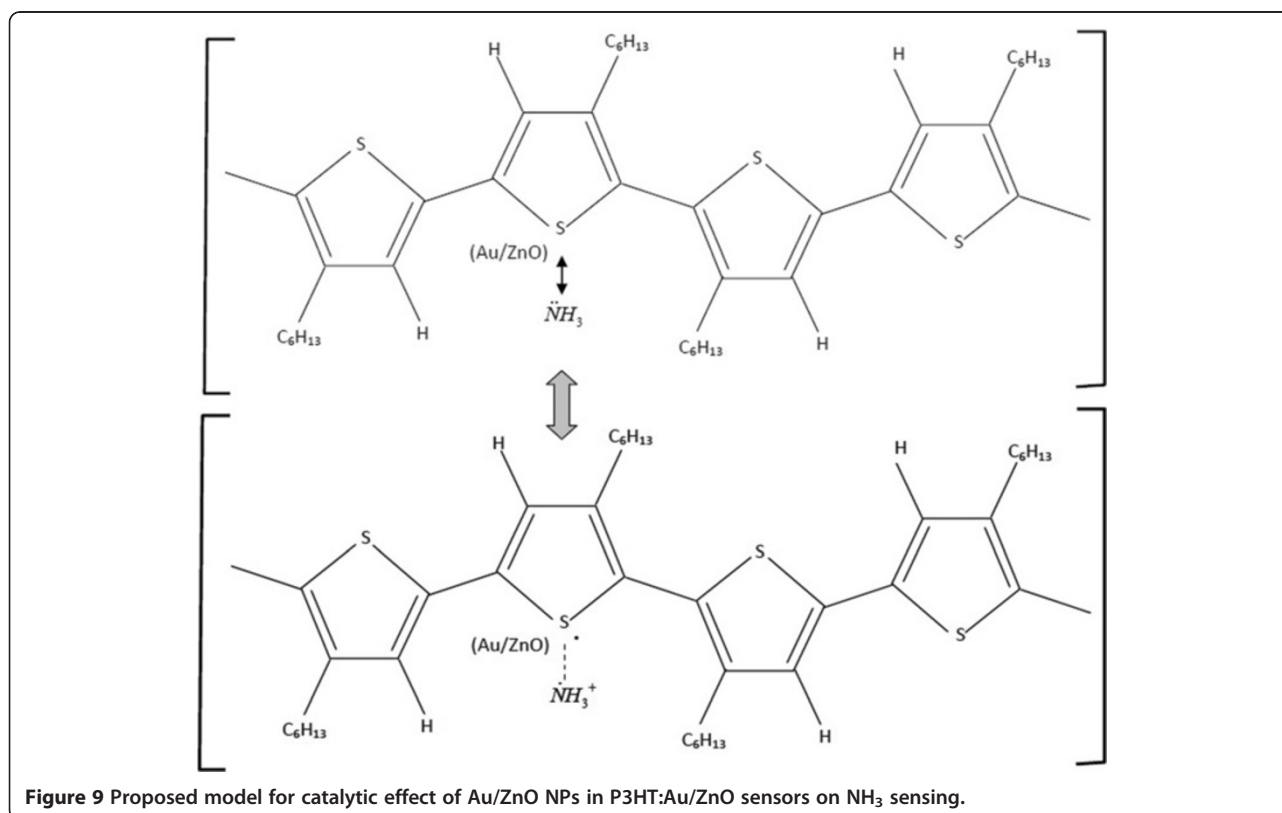


Figure 9 Proposed model for catalytic effect of Au/ZnO NPs in P3HT:Au/ZnO sensors on NH₃ sensing.

Selectivity can be defined as the ability of a sensor to respond to a target gas in the presence of other interfering gases [12]. The NH₃ sensing selectivity of composite sensors is characterized toward various reducing and oxidizing gases including ethanol (C₂H₅OH), carbon monoxide (CO), hydrogen sulfide (H₂S), and nitrogen dioxide (NO₂) at 1,000 ppm and room temperature as shown in Figure 10. In addition, the effect of water vapor is included at 80% RH. It is evident that the composite sensor of P3HT:1.00 mol% Au/ZnO NPs (4:1) exhibits a relatively high response of 32 to 1,000 ppm of NH₃ while the response to 1,000 ppm of C₂H₅OH and NO₂ is relatively low (approximately 9 and approximately 8, respectively), and those of 1,000 ppm of CO and 1,000 ppm of H₂S are almost negligible. Additionally, the optimal sensor exhibits a quite low response of approximately 2.2 to a high relative humidity of 80%. For P3HT and other composite combinations, the response to 1,000 ppm of NH₃ is not much higher than that to C₂H₅OH, NO₂, and humidity. The results indicate that P3HT:1.00 mol% Au/ZnO NPs also has better selectivity to NH₃ against C₂H₅OH, CO, H₂S, NO₂, and humidity than other sensors. Therefore, the composite sensor of P3HT:1.00 mol% Au/ZnO NPs (4:1) can be used for selective detection of NH₃.

Lastly, the stability of P3HT-based sensors has been evaluated by monitoring the response change over 30 days. It was found that the pure P3HT sensor had an average response reduction of around 4.8%/day, while P3HT with 1.00 mol% Au/ZnO NPs and unloaded ZnO NPs at different ratios exhibits slightly lower average response reduction in the range of 4.2% to 4.6%/day. It is not conclusive whether ZnO NPs help improve the stability of P3HT sensors. Nevertheless, it is seen that the ZnO NPs:P3HT sensor has fair medium-term stability,

which is relatively high compared with other conductive polymers.

Conclusions

In conclusion, novel composite P3HT:1.00 mol% Au/ZnO NPs films have been systemically studied for NH₃ sensing applications at room temperature. The unloaded ZnO and ZnO NPs loaded with Au (1.00 mol%) were produced by a single-step FSP technique. The particle analyses using XRD, HR-TEM, and BET indicated that ZnO NPs were highly crystalline with a typical hexagonal structure of ZnO, and ultrafine Au NPs with 1 to 2 nm in diameter were formed around ZnO NPs. Composite P3HT:1.00 mol% Au/ZnO NPs films with different compositions were prepared by solution mixing and casting. Film characterizations by XRD and FE-SEM confirmed the presence of P3HT/ZnO phases and porous nanoparticle structures in the composite thick film. The gas sensing results showed that the inclusion of 1.00 mol% Au/ZnO NPs at a low content provided significant NH₃ sensing enhancement. In particular, the P3HT:1.00 mol% Au/ZnO NPs composite film with the ratio of 4:1 exhibited the best NH₃ sensing performances with a high sensor response of approximately 32 and short response time within a minute to 1,000 ppm of NH₃ at a room temperature. In addition, the optimal composite film exhibited higher NH₃ selectivity against C₂H₅OH, CO, H₂S, NO₂, and H₂O than other composites as well as P3HT and 1.00 mol% Au/ZnO NPs. The observed composite gas sensing behaviors were explained based on the increased specific surface area by porous blended nanoparticle structure and catalytic effect of Au/ZnO NPs. From overall results, the P3HT:1.00 mol% Au/ZnO NPs composite sensor is a highly promising candidate for the efficient detection of NH₃ at room temperature.

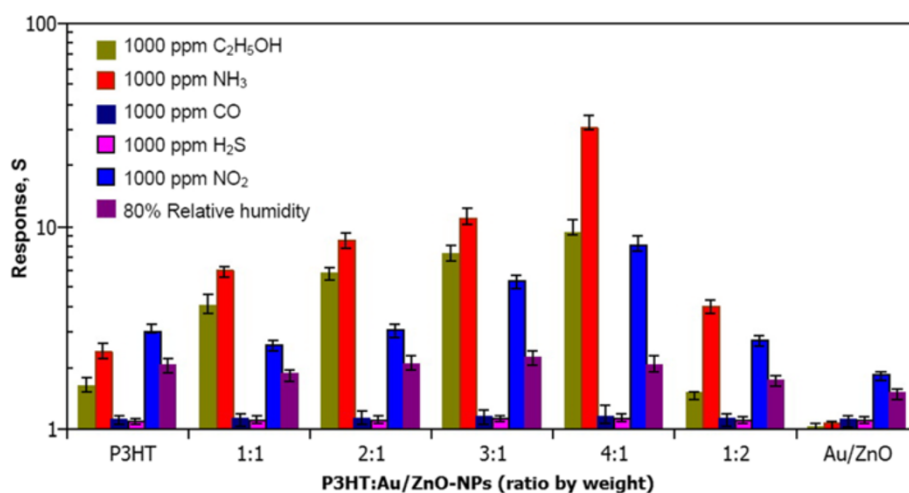


Figure 10 Relative response. The relative response to NH₃ (1,000 ppm), C₂H₅OH (1,000 ppm), CO (1,000 ppm), H₂S (1,000 ppm), NO₂ (1,000 ppm), and H₂O (80% RH) of sensors with difference ratio of P3HT:1.00 mol% Au/ZnO NPs (1:0, 1:1, 2:1, 3:1, 4:1, 1:2, and 0:1).

Abbreviations

AFM: atomic force microscopy; BET: Brunauer-Emmett-Teller; EDX: energy-dispersive X-ray; FE-SEM: field-emission scanning electron microscopy; FSP: flame spray pyrolysis; HR-TEM: high-resolution transmission electron microscopy; NPs: nanoparticles; P3HT: poly (3-hexylthiophene); SSA_{BET} : specific surface area; XRD: X-ray diffraction.

Competing interests

The authors declare that they have no competing interests.

Authors' contributions

VK carried out the experiments, acquired the original data, participated in the sequence alignment, and drafted the manuscript. AW and SP have made substantial contributions to the conception and design for this article. AT read the final manuscript. All the authors read and approved the final manuscript.

Acknowledgements

The authors gratefully acknowledge the financial support from the Thailand Research Fund (TRF), the Office of the Higher Education Commission and Maejo University, Thailand (MRG5580067); Program in Materials Science, Faculty of Science, Maejo University, Thailand; the National Research Council of Thailand; the National Research University under the Office of Higher Education Commission; Materials Science Research Center, Faculty of Science, Chiang Mai University, Thailand; and National Electronics and Computer Technology Center (NECTEC), Pathumthani, Thailand.

Author details

¹Program in Materials Science, Faculty of Science, Maejo University, Chiang Mai 50290, Thailand. ²National Electronics and Computer Technology Center, Pathumthani 12120, Thailand. ³Materials Science Research Center, Faculty of Science, Chiang Mai University, Chiang Mai 50200, Thailand.

Received: 19 May 2014 Accepted: 26 August 2014

Published: 4 September 2014

References

1. Narasimhan LR, Goodman W, Kumar C, Patel N: Correlation of breath ammonia with blood urea nitrogen and creatinine during hemodialysis. *Proc Natl Acad Sci U S A* 2001, **98**:4617–4621.
2. de la Hoz RE, Schueter DP, Rom WN: Chronic lung disease secondary to ammonia inhalation injury: a report on three cases. *Am J Ind Med* 1996, **29**:209–214.
3. Leung CM, Foo CL: Mass ammonia inhalation burns-experience in the management of patients. *Ann Acad Med Singapore* 1992, **21**:624–629.
4. Michaels RA: Emergency planning and acute toxic potency of inhaled ammonia. *Environ Health Perspect* 1999, **107**:617–627.
5. Close LG, Catlin FI, Cohn AM: Acute and chronic effects of ammonia burns on the respiratory tract. *Arch Otolaryngol* 1980, **106**:151–158.
6. Shimizu K, Chinzei I, Nishiyama H, Kakimoto S, Sugaya S, Matsutani W, Stasuma A: Doped-vanadium oxides as sensing materials for high temperature operative selective ammonia gas sensors. *Sens Actuators B Chem* 2009, **141**:410–416.
7. Sun F, Hu M, Sun P, Zheng J, Liu B: NH₃ sensing characteristics of nano-WO₃ thin films deposited on porous silicon. *J Nanosci Nanotechnol* 2010, **10**:7739–7742.
8. Jimenez I, Centeno MA, Scotti R, Morazzoni F, Arbiol J, Cornet A, Morante JR: NH₃ interaction with chromium-doped WO₃ nanocrystalline powders for gas sensing application. *J Mater Chem* 2004, **15**:2412–2420.
9. Balamurugan C, Bhuvanalogini G, Subramania A: Development of nanocrystalline CrNbO₄ based p-type semiconducting gas sensor for LPG, ethanol and ammonia. *Sens Actuators B Chem* 2012, **168**:165–171.
10. Tulliani JM, Cavalieri A, Musso S, Sardella E, Geobaldo F: Room temperature ammonia sensors based on zinc oxide and functionalized graphite and multi-walled carbon nanotubes. *Sens Actuators B Chem* 2011, **152**:144–154.
11. Kolmakov A, Moskovits M: Chemical sensing and catalysis by one-dimensional metal-oxide nanostructures. *Annu Rev Mater Res* 2004, **34**:151–180.
12. Patil LA, Sonawane LS, Patil DG: Room temperature ammonia gas sensing using MnO₂-modified ZnO thick film resistors. *J Model Phys* 2011, **2**:1215–1221.
13. Chougule MA, Sen S, Patil VB: Polypyrrole-ZnO hybrid sensor: effect of camphor sulfonic acid doping on physical and gas sensing properties. *Synth Met* 2012, **162**:1598–1603.
14. Tuan CV, Tuan MA, Hieu NV, Trung T: Electrochemical synthesis of polyaniline nanowires on Pt interdigitated. *Curr Appl Phys* 2012, **12**:1011–1016.
15. Chen X, Li DM, Liang SF, Zhan S, Liu M: Gas sensing properties of surface acoustic wave NH₃ gas sensor based on Pt doped polypyrrole sensitive film. *Sens Actuators B Chem* 2013, **177**:364–369.
16. Jeong JW, Lee YD, Kim YM, Park YW, Choi JH, Park TH, Soo CD, Won SM, Han IK, Ju BK: The response characteristics of a gas sensor based on poly-3-hexylthiophene thin-film transistors. *Sens Actuators B Chem* 2010, **146**:40–45.
17. Tiwari S, Kumar S, Joshi L, Chakrabarti P, Takashimac W, Kaneto K, Prakash R: Poly-3-hexylthiophene based organic field-effect transistor: detection of low concentration of ammonia. *Sens Actuators B Chem* 2012, **171**–172:962–968.
18. Baratto C: *Proceeding of the 5th IEEE Conference on Sensors: IEEE Sensors 2006, 22–25 October 2006*. Daegu, South Korea: 2006.
19. Athawale AA, Bhagwat SV, Katre PP: Nanocomposite of Pd-polyaniline as a selective methanol sensor. *Sens Actuators B Chem* 2006, **114**:263–267.
20. Kruefu V, Liewhiran C, Wisitsoraat A, Phanichphant S: Selectivity of flame-spray-made Nb/ZnO thick films towards NO₂ gas. *Sens Actuators B Chem* 2011, **156**:360–367.
21. Tai H, Juang Y, Xie G, Yu J, Chen X, Ying Z: Influence of polymerization temperature on NH₃ response of PANI/TiO₂ thin film gas sensor. *Sens Actuators B Chem* 2008, **129**:319–326.
22. Ai X, Anderson N, Guo JC, Kowalik J, Tolbert LM, Lian TQ: Ultrafast photoinduced charge separation dynamics in polythiophene/SnO₂ nanocomposites. *J Appl Chem B* 2006, **110**:25496–25503.
23. Dhingra M, Kumar Shrivastava S, Kumra PS, Annapoorni S: Impact of interfacial interactions on optical and ammonia sensing in zinc oxide/polyaniline structures. *Bull Mater Sci* 2013, **36**:647–652.
24. Tsai TH, Lin KC, Chen SM: Electrochemical synthesis of poly (3,4-ethylenedioxythiophene) and gold nanocomposite and its application for hypochlorite sensor. *Int J Electrochem Sci* 2011, **6**:2672–2687.
25. Chang SJ, Weng WY, Hsu CL, Hsueh TJ: High sensitivity of a ZnO nanowire-based ammonia gas sensor with Pt nano-particles. *Nano Commun Netw* 2010, **1**:283–288.
26. Huang X, Hu N, Gao R, Yu Y, Wang Y, Yang Z, Kong E, Wei H, Zhang Y: Reduced graphene oxide-polyaniline hybrid: preparation, characterization and its applications for ammonia gas sensing. *J Mater Chem* 2012, **22**:22488–22495.
27. Saxena V, Aswal DK, Kaur M, Koiry SP, Gupta SK, Yakhmi JV: Enhanced NO₂ selectivity of hybrid poly (3-hexylthiophen): ZnO-nanowire thin films. *Appl Phys Lett* 2007, **90**:043516–1–043516–3.
28. Lima JPH: *Proceeding of the International Conference on Advanced Materials: Brazil-MRS, 20–25 September 2009*. Rio de Janeiro, Brazil: 2009.
29. Wang H, Xie C, Zhang W, Cai S, Gui Z, Hazard J: Comparison of dye degradation efficiency using ZnO powders with various size scales. *J Hazard Mater* 2007, **141**:645–652.
30. Chang SJ, Hsueh TJ, Chen IC, Huang BR: Highly sensitive ZnO nanowire CO sensors with the adsorption of Au nanoparticles. *Nanotechnology* 2008, **19**:1–5.
31. Wongrat E, Pimpang P, Chooon S: Comparative study of ethanol sensor based on gold nanoparticles: ZnO nanostructure and gold: ZnO nanostructure. *Appl Surf Sci* 2009, **256**:968–971.
32. Yu HF, Qian DW: Characterization and photocatalytic kinetics of the ZnO powder prepared using a polyol process. *Part Sci Technol* 2013, **31**:482–487.
33. John R, Rajakumari R: Synthesis and characterization of rare earth ion doped nano ZnO. *Nano Micro Lett* 2012, **4**:65–72.
34. Hua Q, Shi F, Chen K, Chang S, Ma Y, Jiang Z, Pan G, Huang W: Cu₂O-Au nanocomposites with novel structures and remarkable chemisorption capacity and photocatalytic activity. *Nano Res* 2011, **4**:948–962.
35. Lee JS, Kim HS, Park NK, Lee TJ, Kang M: Low temperature synthesis of α -alumina from aluminum hydroxide hydrothermally synthesized using [Al (C₂O₄)_x (OH)_{3-x}] complexes. *Chem Eng J* 2013, **230**:351–360.
36. Pawar SG, Patil SL, Chougule MA, Raut BT, Godase PR, Mulik RN, Sen S, Patil VB: New method for fabrication of CSA doped PANI (TiO₂) thin-film ammonia sensor. *IEEE Sens J* 2011, **11**:2980–2985.

doi:10.1186/1556-276X-9-467

Cite this article as: Kruefu et al.: Gas sensing properties of conducting polymer/Au-loaded ZnO nanoparticle composite materials at room temperature. *Nanoscale Research Letters* 2014 **9**:467.